JMBFS
Journal of Microbiology, Biotechnology and Food Sciences
International peer-reviewed scientific online journal

Published by Faculty of Biotechnology and Food Sciences

CHARACTERIZATION AND EVALUATION OF SOME BIOLOGICAL ACTIVITIES OF SILVER NANOPARTICLES SYNTHESIZED USING *Trigonella foenum graecum* LEAVES' EXTRACT

K. Sobha[1], BRS Srinivas Gupta[1], K Mohan Karthikeya[1], K. Surendranath[2]

Address(es):
[1] Department of Biotechnology, RVR & JC College of Engineering, Guntur 522 019, Andhra Pradesh, India.
[2] Department of Physics, RVR & JC College of Engineering, Guntur 522 019, Andhra Pradesh, India.

*Corresponding author: sobhakota2005@gmail.com

https://doi.org/10.55251/jmbfs.4255

ARTICLE INFO

Received 23. 1. 2021
Revised 8. 2. 2024
Accepted 28. 2. 2024
Published 1. 4. 2024

Regular article

OPEN ACCESS

ABSTRACT

The green synthesized silver nanoparticles (AgNPs) with the aqueous extract of the leaves of household vegetable, *Trigonella foenum-graecum* were characterized and tested for their anti-oxidant and anti-bacterial efficacy with sixteen human clinical isolates. The Formation of AgNPs was confirmed with the surface plasmon spectra of the dark brown solution centered at 448 nm. The Particle size calculated with XRD data was 41.23 nm and the SEM size ranged between 52.56 nm and 80.51 nm. The presence of -NH and -OH groups that effectively react and reduce Ag^+ ions to Ag^0 was evident from the FT-IR spectra. The particles are predominantly spherical in shape and varied from 5 to 80 nm in size. As Suggested from the analysis by SEM and TEM, majority of them fall between 5 nm and 20 nm. A composite solution of AgNPs with polyvinyl alcohol (PVA) was electrospun into films and tested on 8 human clinical isolates including methicillin-resistant *Staphylococcus aureus* (MRSA). The PVA-AgNP films showed enormous activity against the MRSA prompting further study as wound dressings in the Wistar albino rat model. Although the animal study was abruptly terminated owing to the pandemic-induced lock down, the preliminary study results for 9 days suggest the potential clinical applications of these wound dressings. The synthesized AgNPs with and without PVA demonstrated good anti-oxidant activity and highly significant (P = 0.001) zones of inhibition with eighteen clinical isolates were tested.

Keywords: Silver nanoparticles, *T. foenum-graecum*, Green synthesis, Anti-oxidant activity, Antimicrobial activity, Wound healing

INTRODUCTION

Nanoparticles (NPs) /Nanomaterials (NMs) offer solutions in a wide array of disciplines encompassing the domains of energy, health and environment. A Larger surface/volume ratio of NPs is an important attribute for the whole gamut of applications, essentially in catalysis and anti-microbial properties. AgNPs (silver NPs) are of great significance in diverse fields like spectrally selective coatings for efficient absorption of different wavelengths of light, intercalation material for electrical batteries, optical receptors for bio-labeling, and antimicrobial materials in the health care industry **(Florence et al., 2013)**. NPs, with a minimum of one of the three dimensions less than 100 nm, have unique physico-chemical characteristics as compared to the bulk material. Nanoparticles with their enhanced properties under morphology (Size & Shape) and distribution, in contrast to their bulk material characteristics, make a significant contribution for applications in pharmaceutics, food, environment, mechanics, optics, electronics, chemical & space industries, and various photochemical applications **(Shakeel Ahmed et al., 2016)**. A multitude of applications of biosynthesized silver nanoparticles such as formulation of nano-drugs, disinfecting agents in water purification, surface plasmon resonance enhancers, and nano-weapons to kill phyto-pathogenic agents like bacterial and fungi **(Abdelghany et al., 2018)**. Inhibitory potential of silver nanoparticles on the growth, morphology and biomolecular dynamics of the cells of two phytopathogens viz. *Fusarium culmorum* and *Alternaria alternate* were investigated and the results indicate their promising application as a fungicide in agriculture **(Ganash et al., 2018)**. *Juniperus procera*, an African pencil-cedar tree extract with the AgNPs was evaluated for its anti-fungal properties against *Aspergillus flavus* and the aflatoxins produced by the fungus **(Abdelghany et al., 2020)**. The findings reveal the synergistic effects of the plant phytochemicals and the silver nanoparticles in depressing the growth as well as aflatoxin production. Biomedical advantages of copper doped nanocomposites of starch were highlighted in the research study by **Hasanin et al. (2021)**. The study demonstrated the enormous potential of CuNP-starch based nanocomposite as an anti-bacterial, anti-fungal, anti-oxidant and anti-cancerous biomaterial for biomedical use. As the industrial demands are on the rise, efforts are made to switch over to environmentally friendly biological materials for reduction of Ag^+ ions to Ag^0, rather than toxic chemical mediated synthesis. With the imperative need for green synthesis of nanomaterials **(Mandal et al., 2006)** for varied applications, this study was attempted with the aqueous extract of *Trigonella foenum-graecum*, a widely consumed leafy vegetable. The anti-oxidant, anti-microbial and wound healing capability of the synthesized silver nanoparticles were evaluated.

MATERIALS AND METHODS

All chemicals/reagents used in the current study were of analytical grade, purchased from Merck, India. Medium components used for microbiological studies were purchased from Hi-Media, Mumbai, India. Deionized water purchased from a local surgical shop was used for the preparation of all reagent solutions.

Preparation of leaf extract for green synthesis of AgNPs

Young shoots of Fenugreek, *Trigonella foenumgraecum*, were procured from the local vegetable vendor, Guntur, Andhra Pradesh, India, and then washed two to three times to remove soil particles followed by air drying in shade. Leaves of 50 g were macerated, boiled for 15 minutes in 250 ml deionized water, filtered first through muslin fabric and then using grade 1 qualitative (Whatman) filter paper. Standard procedures **(Trease and Evans, 1989)** were adopted for phytochemical analysis of the filtered leaf extract. The extract with pH adjusted to 7.5 was utilized within 3 hours for making silver nanoparticles from silver nitrate solution. Leaf extract was added to 6mM $AgNO_3$ solution in the ratio of 1:10 ml and kept aside for 30 to 60 minutes for the colour to change to brown. After the appearance of dark brown color, the solution was centrifuged at 10K rpm for a period of 20 minutes, collected the pellet and kept in a hot air oven at 60 ^{0}C for about 12 hours for removal of moisture. Finally, the dried pellet was powdered using mortar and pestle and stored in sealed eppendorf tubes at room temperature. For microbiological studies, the AgNPs were autoclaved at 121^{0}C and 15 psi for 20 minutes.

Characterization of AgNPs

The prepared AgNPs were evaluated by UV-Visible spectra obtained by UV-vis spectrophotometer (Elico SL129) at the wavelength of 380 to 500 nm. Using the KBr pellet method, Fourier transform infrared (FT-IR) spectra were obtained in the wave number range of 400 to 4000 cm^{-1} to determine the functional groups. X-ray diffractometer (PANlytical Xpert Pro) equipped with a CuKa radiation source

was used at a generator setting of 40kV/30mA and data was collected varying the 2θ angle between 9.971^0 and 99.955^0 for examining the metallic AgNPs. For the elemental composition analysis by EDAX, a little quantity of the powder was spread on the carbon tape and inserted into the chamber. To infer the morphology and chemical constitution, images were taken in tandem (system Quanta Inspect F), varying the voltages and magnifications. The size ranges of AgNPs were determined from TEM analysis. Powdered AgNPs of 50 mg were placed in a small crucible of alumina (Universal V4.5A TA instrument with model number SDT 2600 V20.9 Build 20) and analyzed by thermo-gravimetric-differential scanning calorimetry (TGA-DSC) using inert N_2 gas, at temperatures ranging from RT (room temperature) to 1000^0 C with a ramp of 20 ^{0}C/min (heating).

Anti-oxidant activity

DPPH radical scavenging

The assay with DPPH was performed following the protocol as given by **Hsu et al. (2007)**. A 5 ml reaction mixture was set up by mixing deionized water, 0.3 mM DPPH in methanol and silver nanoparticles in five different concentrations (40, 80, 120, 160, and 200 µg/ml) in the proportions of 2.5 ml, 1.5 ml and 1 ml respectively, vortexed and allowed to stand for 30 minutes in the dark at surrounding temperature. A blank containing the same reactants except for DPPH was run for each reaction tube, and its absorbance was deducted from the experimental samples' absorbance for correction. The absorbance of the reduced DPPH free radical was read at 517 nm with a spectrophotometer (Elico SL129) of UV-vis range. A control tube containing deionized water and 0.3 mM DPPH in the v/v proportion of 2.5 ml and 1.5 ml respectively was set up simultaneously along with the experimental tubes. Ascorbic acid was run as a positive control, and the percent inhibition of DPPH was determined from the measured values of absorbance using the formula:
Free radical scavenging (%) (by DPPH) = $(A_0 - A_1)/A_0$ X 100 where A_0 and A_1 represent the OD of the control and the test/standard respectively. A graph was plotted with % scavenging activity Vs. AgNP concentration and the equation obtained was used for the calculation of IC_{75} **(Rahman et al., 2019)**.

Hydrogen peroxide scavenging

Ruch et al. (1989) method with a few modifications was employed for estimation of hydrogen peroxide scavenging by the AgNPs. In the first step, 40 mM strength of H_2O_2 was prepared in 0.1M phosphate buffer solution (PBS) (pH 7.4) and a 0.6 ml of it was added to reaction tubes containing 3.4 ml of PBS with specified quantities of AgNPs (40, 80, 120, 160, and 200 µg/ml), suspended in equivolume mixture of methanol and water, and incubated for 10 minutes. In the place of silver nanoparticles, the standard samples contained similar concentrations of ascorbic acid. OD of the test solution was measured at 230 nm against phosphate buffer as a blank and the extract containing specified concentrations of AgNPs, without H_2O_2. The OD of 40 mM hydrogen peroxide served as a control. The H_2O_2 radical scavenging activity in (%) was calculated as:
H_2O_2 radical scavenging activity (%) = $(A_0 - A_1) / A_0$ X 100
where A_0 and A_1 denote the OD of the control and the test/standard respectively. Using the regression equation of the plot between scavenging activity % and AgNP concentration, the IC_{75} value was calculated.

Reducing power assay

Each of the five concentrations of AgNPs viz. 40, 80, 120, 160, and 200 µg/ml were suspended in an equivolume mixture of methanol: water and tested for reducing power by the proposed method of Oyaizu (1986). A volume of 1 ml for each of the concentrations of the sample was added to a reaction mixture comprising 2.5 ml of 0.2M PBS (pH 6.6) and 2.5 ml of 1% potassium ferricyanide. An incubation time of 20 min at 50^0C in a hot water bath was provided. Then, the contents were added with 2.5 ml of 10% TCA (trichloroacetic acid) and centrifuged for 10 min at 3000 rpm. Finally, a precisely measured 2.5 ml of the top layer of the solution was collected, added to 2.5 ml of distilled water and 0.5 ml of ferric chloride in the test tube and absorbance was measured using the UV-Vis spectrophotometer (Elico SL129) at 700 nm. A blank containing all the reagents except the sample was run simultaneously. A stronger absorbance is indicative of higher reducing power.

Nitric oxide scavenging

Nitric oxide (NO) synthase enzymes specifically metabolize amino acids like arginine and generate nitric oxide free radicals ($NO^{\cdot}$) in the cells. Free radicals of NO in aqueous solution released by the decomposition of sodium nitroprusside at a pH of 7.2 were determined by Griess reagent (Marcocci et al., 1984). This *in vitro* reaction was employed to determine the NO scavenging potential of the AgNPs. The reaction was set up by adding 0.5 ml suspension of specific amounts of AgNPs (40, 80, 120, 160, and 200 µg/ml) in 1:1 methanol: water to 2 ml of 10mM sodium nitroprusside dissolved in 0.5 ml PBS (pH 7.4). The contents were then kept for incubation at 25 ± 2^0C for 150 minutes and absorbance was noted at 546 nm for all the test samples that also served as control. From the freshly prepared Griess reagent containing equal quantities of 2% sulphanilamide in 1.47M HCl and 0.1% N-(1-naphthyl ethylenediamine dihydrochloride in deionized water, 2 ml was taken and added to 2 ml each of the incubated test samples, and kept for incubation for 30 min at room temperature. Absorbance at 546 nm was measured for the second time after incubation with Griess reagent and $NO^{\cdot}$ inhibition in percent was determined as:

$$\text{Inhibition of NO radical (\%)} = [A_0 - A_t]/A_0 \text{ x } 100$$

where A_0 and A_t denote respectively the absorbance values before and after reaction with Griess reagent. As mentioned earlier, from the regression equations, the IC75 values in µg/ml for AgNPs and the ascorbic acid standard were calculated and given in Table 3.

Anti-Bacterial activity

Initially, the potential of the prepared silver nanoparticles was evaluated against 16 human clinical bacterial isolates procured from patients of two local multi-specialty hospitals viz. NRI Medical College Hospital, Mangalagiri, and Katuri Medical College Hospital, Chowdavaram of Guntur district, Andhra Pradesh. The clinical isolates were cultured on a solid nutrient medium (Himedia) containing 3g of yeast extract, 5g of peptone, 5g of NaCl, and 15g of Agar in 1L of distilled water with pH 7.2 at 37^0C for 24 hrs with aerobic conditions maintained. Antibacterial activity was assessed with the cultured cells after 2 passes using the agar well diffusion method. Nutrient agar culture plates were prepared by pouring 15 ml of slightly warm molten agar from sterile conical flasks, mixed gently with 0.2 ml of bacterial culture before dispensing. Wells in the solidified agar were punched with a sterilized cork borer in the petriplates. Then 10 µl, 20 µl and 30 µl of AgNPs suspended as 50 mg/ml in water were added to wells whose bases were sealed with agar and the extra well with 5% DMSO served as a control. After incubation of the culture plates at 37^0C for 24 hrs, inhibition zones were measured (using the Himedia antibiotic zone scale) in mm (Fig. S4a to S4c). The averages of the zones obtained with ± S.D. are reported in Table 4.

Preparation of composite films impregnated with AgNPs

Polyvinyl alcohol (PVA), a unique water-soluble synthetic polymer with excellent biocompatibility, with safety and FDA approval, has good mechanical and thermal properties as well as good transparency and resistance to O_2 permeation. Further, its decomposition rate is low in certain environments with the least resistance to water because of the hydroxyl groups in the repeating units of PVA (Gupta et al., 2013; Gaaz et al., 2015; Lim et al., 2015; Aslam et al., 2019). The matrical membrane of polyvinyl alcohol (PVA) impregnated with AgNPs was prepared by dissolving 5 g of polyvinyl alcohol (PVA) in a solvent mixture of DI water, ethanol and acetic acid in a 5:3:2 (v/v) ratio and added with 0.5g of AgNPs (synthesized with the leaf extract of *T. foenum-graecum*). The mixture was heated to 80^0C for 2 hours with constant stirring to ensure the complete dissolution of PVA and AgNPs. The material was finally electrospun into fibrous films by applying a voltage of 14 kVa, a flow rate of 2 ml/hr and maintaining a working distance of 14 cm with a drum speed of 700-800 rpm.

Wound healing potential - Excision wound model

For the wound healing studies, the protocol proposed by **Mukherjee et al. (2000)** was followed with a few modifications. Three groups of Wistar albino rats in the weight range of 150-180 grams were chosen for the investigation. In total, 15 animals comprising 5 for each group, were housed in cages and were given feed and water ad libitum. The rats were subjected to experimentation after a period of acclimation for one week. The animals were shaved in and around the region of the proposed wound area using depilatory cream and anesthetized using ketamine hydrochloride (50 mg/kg, i.p., bodyweight). A full-thickness wound by excision with a circular area of 3 x 3 cm^2 was made along the contour of the impression marked using surgical equipment. The control group rats were not given any treatment, the standard group was dressed with a cotton gauge patch containing povidone-iodine solution and in the test group, and the wound was covered with wound dressing containing PVA + AgNP film. The wound dressings were changed on alternate days and the readings were noted just before placing the new dressing. Each wound dressing contained PVA+AgNP film of 5 x 5 cm^2 area (to cover the wound area of 3 x 3 cm^2), layered on top with absorbent cotton and gauge and stuck to the body covering the wound area with micropore surgical paper tape. In this model, the wound contraction period was evaluated. Wound healing in terms of contraction was recorded as percent on day 1, 3, 5, 7 and 9 after wound formation.
Wound area was measured on alternate days by tracing the wound with the help of transparent sheet using millimeter-based graph paper on days 1, 3, 5, 7 and 9 for all groups **(Udupa et al., 1994a; Udupa et al., 1995; Saha et al., 1997)** and percent wound contraction was calculated, taking the initial size of the wound as 100%, using the following formula:

Wound contraction (%) = (Initial wound area − Specific day wound area) / Initial wound area×100.

RESULTS AND DISCUSSION

Characterization

The study was focused on green synthesis of AgNPs with the aqueous leaf infusion of the medicinal herb, *T. foenum-graecum* commonly consumed as a leafy vegetable in every household of India. UV-vis spectra indicating the centering of surface plasmons at 448 nm (Fig. S1) confirmed the presence of AgNPs, similar to the AgNPs synthesized with *R. acetosa* **(Sobha et al., 2017)**. The visible color change from yellow to deep brown within one hour of addition of the leaf extract to the solution of 6mM $AgNO_3$ was due to the excitation of surface plasmon resonance vibrations combined with the metallic silver nanoparticles (Mohan Kumar et al., 2012; Kalairasi et al., 2015; Shankar et al., 2004; Sobha et al., 2017). FT-IR spectral peaks (Fig. S2) demonstrated at 651 and 691 cm^{-1} suggest the C-H & N-H bending vibrations which are out of the plane. The N-H bending vibration is reflected as a sharp peak at 1636 cm^{-1}. The involvement of N-H amines and O-H bonds is reflected by the peaks at 3366 cm^{1}, 3723 cm^{-1}, 3788 cm^{-1}, 3834 cm^{-1}, 3875 cm^{-1}, 3923 cm^{-1}, and 3958 cm^{-1} (Table 1).

Table 1 FT-IR spectral characteristics of the silver nanoparticles synthesized with the leaf extract of *T. foenum-graecum*

S. No.	Absorption Peaks (cm^{-1})	Assigned functional groups
1	651, 691	C-H & N-H out of plane bend; C-X (Halide) strong stretch
2	1636	N-H bend, C=O stretch amide, C=C stretch (alkenes)
3	3366, 3723, 3788, 3834, 3875, 3958	C-H, N-H (amines), O-H bond stretch

The XRD of the prepared sample was recorded using Cu Kα radiation of λ = 1.5418 A^0 and indexed using Joint Committee on Powder Diffraction Standards (JCPDS) card data (Fig. 1). The three peaks 37.89, 64.63, 77.66 are close to the reported Ag 2θ values of 38.29, 64.81 and 77.43 and were indexed as (111), (220) and (311) for the crystalline planes of face-centered cubic (fcc) of Ag NP (JCPDS File No. 04-0783) and the remaining lines 27.722, 32.235, 46.198, 54.66, 57.602 were indexed to (211), (122), (231), (044) and (412) of $AgNO_3$ (JCPDS File No. 43-0649) respectively and the results are in corroboration with the earlier reports on plant-mediated synthesis of AgNPs (Kalairasi et al., 2015; Kayalvizhi et al., 2016; Mohan Kumar et al., 2012; Ponarulselvam et al., 2012; Sobha et al., 2017). The presence of non-reduced $AgNO_3$ is most common in the AgNP preparations made with the plant extracts. With the obtained XRD data (2θ = 32.26; FWHM = 0.2007; Relative intensity = 100%), the size of the particles determined using Scherrer equation (D = 0.9λ/β cos θ) was 41.23 nm, while the measured sizes by SEM were 52.56 nm and 80.51 nm (Fig. 2a). Factors like the phytochemical composition of the plant extract, hydrogen ion strength of the solution, reaction temperature are some of the many that were reported to influence the shape and size of the green synthesized nanoparticles **(Rauwel et al., 2015)** and the same was evident in the current study. The synthesized nanoparticles are demonstrated, by energy dispersive x-ray analysis, to contain significantly high Ag, about 62.52% while C, N, O and Cl corresponded to 4.43%, 5.76%, 19.45% and 7.85% respectively (Fig. 2b; Table 2). These values are in close approximation to what were obtained for AgNPs made by *R. acetosa* extract **(Sobha et al., 2017)** suggesting similarity in the phytochemical composition of edible plant extracts. XPS spectrum also showed distinct, predominant peaks for silver, and others for C, N, O and Cl only.

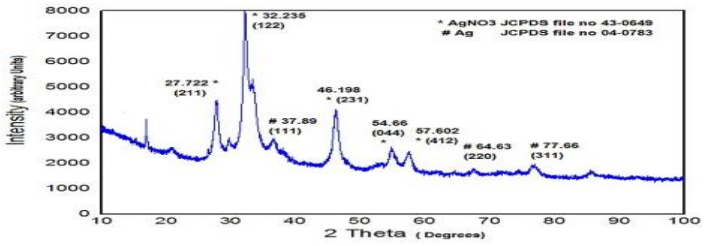

Figure 1 XRD pattern of the crystal structure of the silver nanoparticles obtained by green synthesis with the leaf extract of *T. foenum-graecum.*

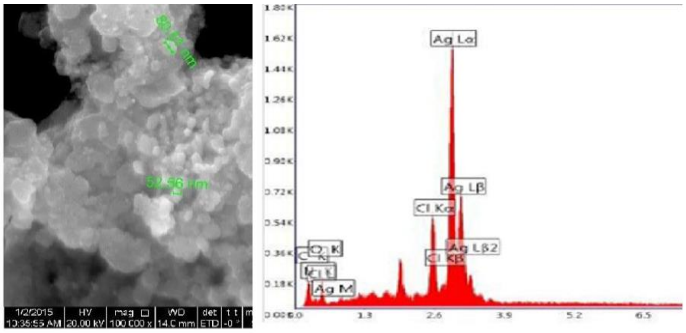

Figures 2a & 2b Micrograph of synthesized silver nanoparticles with the extract of *T. foenum-graecum* obtained by Scanning Electron Microscopy and EDAX showing elemental composition

Table 2 Weight % composition of the synthesized Ag NPs (with *T. foenum-graecum* extract) obtained by EDAX analysis

S. No.	Element	Weight %	Atomic %	Net Intensity	Net Int. Error
1	C K	4.43	13.18	10.22	0.13
2	N K	5.76	14.71	7.63	0.12
3	O K	19.45	43.47	34.07	0.04
4	Cl K	7.85	7.92	144.98	0.03
5	Ag L	62.52	20.73	530.44	0.01

Data from TEM analysis indicated the particles to be predominantly in the size range between 5 and 20 nm; yet the maximum number of particles were in the size range between 10 and 15 nm (Fig. 3a; Fig. S3a & Fig. S3b). These size ranges were less than those obtained in our earlier work with the leaf extract of *R. acetosa* (Sobha et al., 2017). In summary, the AgNPs obtained with the leaf infusion of *T. foenum-graecum* are inferred, from SEM and TEM data, as spherical and in the broad size range of 10nm to 20nm while the maximum size was 80.5 nm. The HRTEM analysis was done using the Gaton digital micrograph to calculate the inter-planar distance, and found it to be between 0.2346 nm and 0.242nm, suggesting the occurrence of AgNPs (Fig. 3b). The morphological attributes of the particles, as indicated by the lattice fringes and SAED pattern, are highly crystalline and spherical in nature. AgNPs synthesized with the ethanolic extract of crushed fruits of *Santalum album* were reported to have FCC structure with an average crystalline size (D) of 20 nm, interplanar spacing (d) of 1.75 Å between the atoms, lattice constant of 4.0676 Å as against the standard value 4.0875 Å for silver and cell volume 67.35 Å (Mehta et al., 2017).

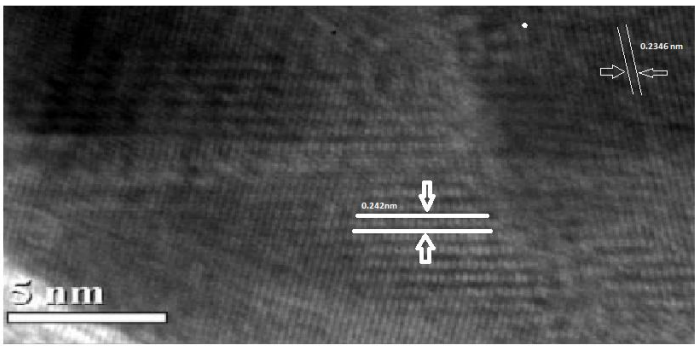

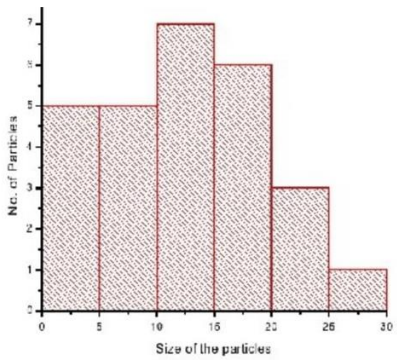

Figures 3a & 3b Size distribution of silver nanoparticles (nm) synthesized with the leaf extract of *T. Foenum-graecum* and HRTEM showing inter-planar distance

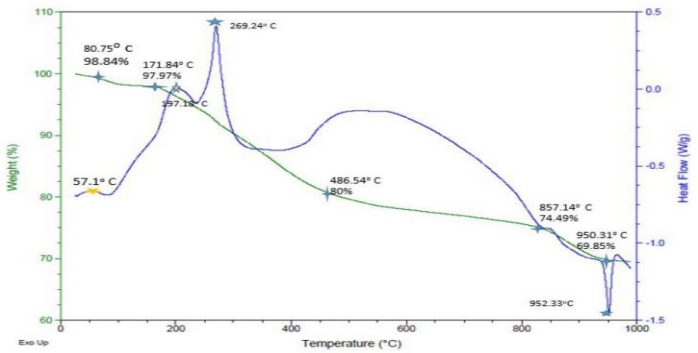

Figure 4 DSC-TGA of the synthesized silver nanoparticles with the leaf extract of *T. foenum- graecum*

The XPS peaks were fitted with Gaussian line shapes and were in reasonably good agreement with the experimental data as shown in the Fig. S3. The C1s curve was deconvoluted as two. From the XPS spectrum (Fig. S4), the peaks with the binding energies 284.61eV and 287.38eV, were corroborated to the carbon atoms of the aliphatic C-C chain and carboxylic Carbon O-C=O respectively. The binding energies of 368.0eV and 374.08eV corresponding to Ag $3d_{5/2}$ and Ag $3d_{3/2}$ respectively with splitting of 6.08eV reflect the formation of carboxylate-protected Ag^{o} metal monolayer protected clusters (Ag MPC). These are slightly different from the Ag NP prepared from leaf extract of *R. acetosa* (Sobha et al., 2017). The very broad peak of O1S with the binding energy of 532.18eV is also slightly different to that of 532.4 eV obtained with *R. acetosa*. This broad peak can be differentiated into three peaks corresponding to C=O (carbonyl and carboxyl, 531.6eV), C-O (532.4eV) and O-H (hydroxyl, 533.35eV) groups. The mass concentration % was 55.66 for Ag 3d, C 1s was 34.92 and O 1s was 9.42 (Table S1).

The thermal stability and the purity of the AgNPs were assessed simultaneously by performing DSC and TGA analyses. The recorded 950 ^{0}C melting point of AgNPs is nearer to that of the reported metallic silver of 960.54 ^{0}C, confirming the purity of the particles. The TGA curve (Fig. 4) showed a total weight loss of 30.29%, indicative of the capping of AgNPs by phyto – organic compounds which appear to degrade in the temperature range of 170 ^{0}C to 500 ^{0}C. The first derivative of TGA (Fig. S5) curve had shown peaks at 70 ^{0}C, 270 ^{0}C, 390 ^{0}C and 860 ^{0}C respectively that confirmed the four-step weight loss process. The first peak may be attributed to the loss of moisture, the second peak at 270 ^{0}C could probably be due to the decomposition of capped phyto – organic compound which coincides with one of the DSC exothermic peaks. The DSC curve had shown two exothermic peaks, one at 197.18 ^{0}C and the other at 269.24 ^{0}C which can be due to the decomposition of capped phyto- organic molecules to the AgNPs at different sites. The broad hump centered around 550 ^{0}C may be an indication for the melting of unreacted $AgNO_3$. The endothermic peak at 952.33 ^{0}C is due to melting of the Ag(0) particles.

Antioxidant activity

The anti-oxidant effects of AgNPs prepared with *T. foenum-graecum* were investigated *in vitro*. DPPH, H_2O_2 and NO scavenging abilities together with reducing power were estimated and the regression equations plotted (Fig. 5a to 5d). All the measured activities were in linear relationship with the concentrations of the AgNPs but significantly different from what was obtained with ascorbic acid used as standard. The AgNPs demonstrated significantly lower activity for DPPH and Reducing power assays as compared with the ascorbic acid (standard), but were in good agreement with the standard in the cases of NO and H_2O_2 scavenging activities. The AgNPs demonstrated statistically highly significant H_2O_2 scavenging, better than ascorbic acid. The calculated IC_{75} values also demonstrate that the AgNPs possess higher scavenging activity (lower concentration) than Ascorbic acid with H_2O_2, while in the remaining cases, the efficiency was in the decreasing order of NO, DPPH and reducing power activities (Table 3). These findings are in consensus with our earlier studies involving the leaf extracts of *R. acetosa*. However, our results are in sharp contrast with one recently reported result for DPPH and H_2O_2 scavenging in which AgNPs performed better than ascorbic acid in scavenging DPPH (29.55% Vs. 24.28%) and not with H_2O_2 (45.41% Vs. 65.63%) (Keshari et al., 2020). In general, natural extracts tend to show lesser activity because of complex compositions and the occurrence of interfering substances as opposed to standards of high purity. Reports on the anti-oxidant activity of plant tissue extracts and/or AgNPs synthesized with them **(El Rafie and Hamed, 2014; Kanipandian et al., 2014; Kharat et al., 2016; Parveen et al., 2016)** indicate that two phytoconstituents viz. phenolics and flavonoids are responsible for the antioxidant activity (Saumya and Basha, 2011), more particularly the phenolics (Philip, 2011) as they tend to donate electron facilitating the conversion of $AgNO_3$ to Ag (0) and formation of AgNPs. The statistical results suggest that the AgNPs prepared with phytoextract of *T. foenum-graecum* are a good choice as anti-oxidant therapeutics despite their relatively low potential against some agents like DPPH.

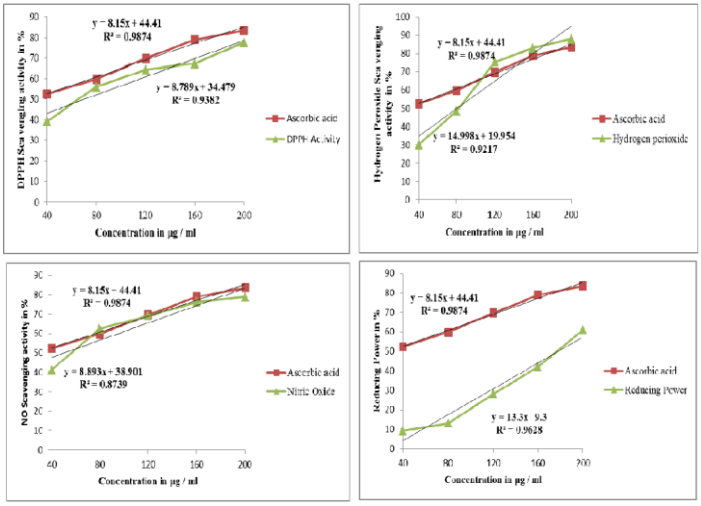

Figures 5a to 5d Anti-oxidant activity of synthesized Ag NPs with *T. foenum-graecum* leaf extract, in comparison with ascorbic acid

Table 3 Calculated IC_{75} values for the synthesized *T. foenum- graecum* derived Ag NPs in comparison with the standard ascorbic acid.

S. No.	Antioxidant Assay	IC_{75} Concentration (µg/ml)		Student's 'T' test		Inference
		Ag NPs	Ascorbic acid	T value	*p* value	
1	DPPH	4.61	3.75	53.0979	0.0001	Highly significant
2	H_2O_2	3.67	3.75	4.9614	0.0011	Highly significant
3	NO	4.06	3.75	18.2038	0.0001	Highly significant
4	Reducing Power	6.34	3.75	73.2563	0.0001	Highly significant

Antibacterial activity

AgNPs are demonstrated to kill bacteria by one or more of the mechanisms viz. pit formation in the rigid cell walls (adhesion), altered cell membrane permeability (Intrusion), free radical production that induces porosity in the cell membrane, enzyme inactivation by the release of free radical species or blocking of thiol groups, destruction to information molecules like DNA, bacteriostasis through blockage of signal transduction are some of the few to be considered (Sharma et al., 2009; Ankanna et al., 2010; Shakeel Ahamed et al., 2016; Abdelghany et al., 2018; Khan et al., 2019). Ag^{+} ions are reported to associate with nucleic acids, through their preferential interaction with nucleosides, and form complexes. The Ag^{+} ions released from AgNPs (Yakabe et al., 1980; Sondi and Sondi, 2004) are reported to get attracted towards negatively charged bacterial cells (Cao et al., 2001), cross the membrane(s) and intrude into the cells by destructing the cell wall and/or cell membranes. Some of the critical physico-chemical parameters like surface charge, concentration, size, shape and colloidal state. affect the anti-microbial potential of AgNPs (Dakal et al., 2016). Biosafety, biocompatibility, efficacy, stability and specificity are some key attributes of AgNPs that are to be tailored through an appropriate methodology of their synthesis, and prevent microbial resistance to AgNPs (Dakal et al., 2016). Recent research demonstrated the anti-oxidant and anti-cancer applications of nanocomposite of starch and fungal-derived CuNPs (Hasanin et al., 2021).

The study included the use of high morbidity inducing clinical isolates of Gram +ve, methicillin-resistant strain of *S. aureus* (MRSA) and the Gram –ve, *Vibrio cholera*, and enterotoxic *Escherichia coli* (ETEC). Multiple drug-resistant *Klebsiella pneumonia, Pseudomonas aeruginosa, Salmonella typhi* were some of the total 18 clinical isolates studied (Salem et al., 2015). Nanda and Saravanan (2009) tested the efficacy of AgNPs against methicillin-resistant *S. aureus* (MRSA), methicillin-resistant *Staphylococcus epidermidis* (MRSE), *S. pyogenes, S. typhi*, and *K. pneumoniae*. The antibacterial activity was observed to be maximum in MRSA, intermediate in MRSE and *S. pyogenes*, while the same effect against *S. typhi* and *K. pneumonia* was moderate.

Antimicrobial activity of nanoparticles has been established with pathogenic bacterial strains of *E. coli* (Yoon et al., 2007) and *S. aureus* (Uparelia et al., 2008). The measured microbial inhibition zones (Fig. 6a to 6f; Fig. S6a to S6c) with the eighteen clinical isolates are provided in Table 4. The AgNPs are active against both Gram-positive and Gram-negative species and the zones varied between ~9 mm (*Escherichia* and *Citrobacteria*) and ~30.4 mm (MRSA).

Figure 6a

Figure 6b

Figure 6c

Figure 6d

Figure 6e

Figure 6f

Figures 6a to 6f Zones of Inhibition obtained with the silver nanoparticles synthesized using the leaf extract of *T. foenum-graecum*

Table 4 Zones of inhibition (mm) obtained with Ag NPs synthesized using the extract of *T. foenum-graecum* and its PVA composite film against human clinical isolates

S. No.	Name of the organism	Gram's reaction and cell morphology	Zone of Inhibition (mean±S.D.) in mm obtained with 50 µg/µl concentration of aqueous suspension of Ag NPs			Zone of Inhibition (mean±S.D) in mm obtained with PVA+AgNP electrospun film
			10 µl	20 µl	30 µl	
1	*Bacillus cereus*	Gram +ve, rod	15.5±0.5	15.5±0.5	15.75±0.75	-
2	*Klebsiella sps.*	Gram –ve, rod	12.5±0.5	12.5±0.5	12.5±0.5	-
3	*Proteus vulgaris*	Gram –ve, rod	17.5±0.5	17±0	17±0	-
4	*Pseudomonas sps.*	Gram –ve, rod	12±0	12±0	14.5±0.5	-
5	*Salmonella paratyphi A*	Gram –ve, rod	14±0	15±0	12.5±1.7	-
6	*Serratia*	Gram –ve, rod	14±1	14.75±0.25	15.5±0.5	-
7	*Shigella dysentery A*	Gram –ve, rod	14.5±0.5	14.5±0.5	15.5±0.5	-
8	*Shigella flexneri*	Gram –ve, rod	15.5±0.5	15.5±0.5	16±0	-
9	*Staphylococcus epidermidis*	Gram +ve, cocci	13.5±0.5	14±0	14.5±0.5	
10	*Vibrio cholera*	Gram –ve, comma shaped	14.7±0.5	15±0	15.7±0.5	-
11	*Enterococcus sps.*	Gram +ve, cocci	16±0	16±0	16.5±0.5	12.6±0.11
12	*Staphylococcus aureus*	Gram +ve, cocci	16±0	16.75±0.25	16.75±0.25	16.9±0.18
13	*Methicillin Resistant Staphylococcus aureus*	Gram +ve, cocci	-	-	-	30.4±0.36
14	*Escherichia coli*	Gram –ve, rod	13.5±0.5	14±0	15±0	8.8±0.21
15	*Proteus mirabilis*	Gram –ve, rod	13±0	13.5±0.5	14±0	7.8±0.08
16	*Salmonella typhi & Salmonella typhimurium*	Gram –ve, rod	13±0	13±0	13.5±0.5	15.6±0
17	*Salmonella paratyphi B*	Gram –ve, rod (Tartrate negative)	-	-	-	13.4±0.1
18	*Citrobacteria*	Gram –ve, Coliform	-	-	-	8.8±0.16

Among the eight clinical isolates (3 are Gram +ve and 5 are Gram –ve) tested with PVA and AgNP electrospun film (Fig. 7a to 7f), *S. typhi*, *S. typhimurium* and methicillin resistive *S. aureus* (MRSA) are maximum inhibited. Of the five Gram negative species tested, *S. typhi /S. typhimurium* are better inhibited than *E. coli, S. paratyphi B, Citrobacteria and P. mirabilis.* With the AgNPs, *Proteus vulgaris, Enterococcus sps. Staphylococcus aureus, Shigella flexneri, Serratia, Shigella dysentery A, Bacillus cereus and Vibrio cholera were strongly inhibited* (Fig.10a to 10f). Although there are variations in the zones of inhibition obtained with different extracts used in the preparation of AgNPs, still the silver nanoparticles made with chemical assistance of biological materials are preferred due to their least/no toxicity to host cells.

Figure 7a

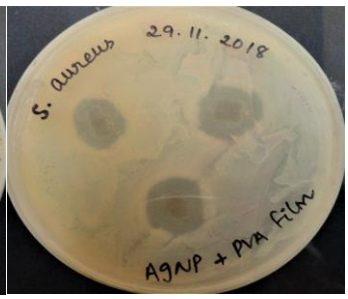

Figure 7b

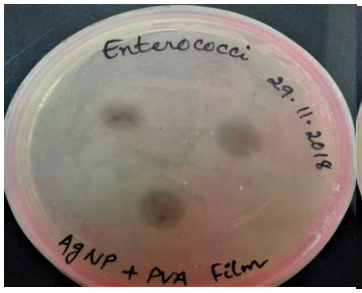

Figure 7c

Figure 7d

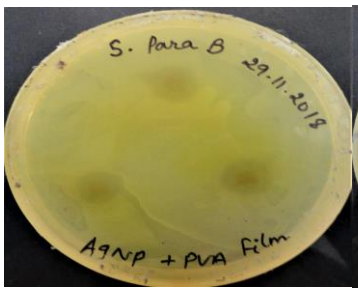

Figure 7e

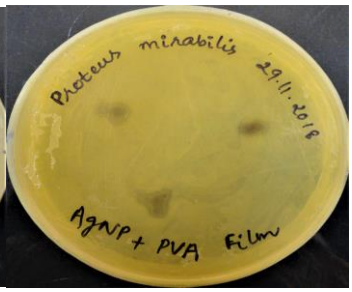

Figure 7f

Figures 7a to 7f Zones of Inhibition obtained with the electrospun film of PVA and silver nanoparticles synthesized using the leaf extract of *T. foenum-graecum*

Wound healing potential

Wound-healing is a complex, dynamic process of several biochemical reactions effected to restore the damaged cellular structure to normalcy (Clark, 1985; Mohammade et al., 2012; Okur et al., 2020). Any wound healing process typically involves three sequential, overlapping phases of inflammation, proliferation and remodeling (Kondo and Ishida, 2010). Plant extracts are reported to be promising natural therapeutic drugs for wound healing because of their diverse, active phytochemical ingredients with minimal or no side effects (Hajialyani et al., 2018). Research reports suggest that AgNPs used in different pharmaceutical formulations like ointments enhance the wound healing process by inhibiting the bacterial growth, or dampening the inflammation process (Jain et al., 2009; Kwan et al., 2011) and/or the growth of fibroblasts by glycosaminoglycans (Im et al., 2010). In the current study, all the three groups demonstrated wound healing but with varying wound reduction rates with time (Table 5; Fig. 8a to 8c). The control group showed no visible healing signs till day 3 but thereafter showed a considerable diminution in the wound area with 6.7, 13.5, 16.9 % reduction on 5th, 7th and 9th day of observations respectively. In the standard group of animals which received a dressing containing povidone-iodine showed a significantly (P=0.001) better wound contraction right from day 3 with 3.2% decrease in wound area to 32.7% on day 9 through 13.1% and 22.9% reductions on day 5 and 7 respectively. There was a highly significant (P=0.0001) wound reduction in test group animals with PVA+AgNP dressings from 12% on day 3 to 46.5% on day 9 through 22.4% and 31% on day 5 and day 7 respectively. As the study ended prematurely due to unavoidable circumstances, further detailed observations till complete wound healing could not be made. However, from these preliminary observations, it could be inferred that a significantly fast wound healing accompanied with the formation of new tissue is facilitated by the silver nanoparticles. In fact, the wound areas were deliberately challenged with laboratory cultures of methicillin-resistive strain of *S. aureus* (MRSA) to check whether similar result obtained in petriplate cultures is repeated in animal model. The customized wound dressing inhibited the infection by MRSA suggesting its potential in containing infections of wounds possibly in human subjects. Research supports the additional benefit of green synthesized AgNPs as they are capped with phytochemical constituents like flavonoids that have anti-viral and anti-bacterial activities (Yang et al., 2008; Hemant Kumar et al., 2016; Keshari et al., 2020). The rupture strength of the treated wounds gradually increased 3rd to 9th day suggesting the formation and stabilization of collagen fibres (Udupa et al., 1995).

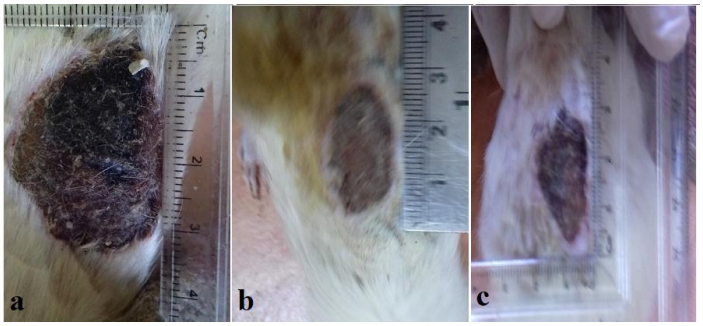

Figures 8a to 8c Control, standard and test animals with excision wound healing in progress as on Day 9 of the Experimentation (a: Control; b: Standard; c: PVA+AgNPs wound dressing)

Table 5 Wound healing studies with PVA+AgNP (with the extract of *T. foenum-graecum*) using wistar albino rats

S. No.	Days	Control (cm^2)	Wound area reduction (%)	'T' test and P values	Povidone-Iodine (cm^2)	Wound area reduction (%)	'T' test and P values	PVA-AgNP patches (cm^2)	Wound area reduction (%)	'T' test and P values
1	1st day	8.85 ±0.21	0		9.15 ±0.21	0		8.7 ±0.42	0	
2	3rd day	8.85 ±0.21	0	**t = 10.1015 P = 0.0097 (Highly Significant)**	8.85 ±0.21	3.2	**t = 20.2031 P = 0.0024 (Highly significant)**	7.65 ±0.21	12.0	**t = 14.9387 P = 0.0001 (Highly significant)**
3	5th day	8.25 ±0.21	6.7		7.95 ±0.21	13.1		6.75 ±.02	22.4	
4	7th day	7.65 ±0.21	13.5		7.05 ±0.21	22.9		6 ±0.42	31.0	
5	9th day	7.35 ±0.21	16.9		6.15 ±0.21	32.7		4.65 ±0.21	46.5	

CONCLUSION

Silver nanoparticles synthesized with the aqueous leaf infusion of *T. foenum-graecum* and characterized by bio-analytical techniques confirmed their formation in the broad size range of 5nm to 80 nm. The anti-oxidant potential was in concord with the standard ascorbic acid, particularly against hydrogen peroxide. Remarkable inhibition of methicillin resistant *S. aureus* was obtained, suggesting potential clinical application in the inhibition of pathogenic Gram –ve and Gram +ve bacteria. Highly significant wound contraction to the extent of 46.5% on day 9 as against 32.7% in standard and 16.9% in control was observed in the rat model challenged with excision wound and tested with wound dressings made of PVA and AgNPs. The experimental results obtained were against the wound and a subsequent deliberate contamination with MRSA. Hence, further studies will aid to check the efficacy of the wound dressings in terms of time taken for complete healing of wound and prevention of sepsis. With the preliminary results obtained, there is a convincing indication that the AgNPs prepared with *T. foenum-graecum* extract could be developed into suitable therapeutic dressings for topical wounds in subjects with injuries like burns. Further work could be directed towards targeted drug delivery of nano-formulations of AgNPs for enhanced bioavailability, controlled and sustained drug release systems.

Funding: This research did not receive any specific grant from funding agencies in the public, commercial, or not-for-profit sectors

Conflicts of interest/competing interests: The authors declare no conflicts of interest / competing interests

Ethics approval: The animal study protocol was approved by the Nirmala college of pharmacy, Mangalagiri, Guntur Dt. AP, India with the protocol approval number: 0S/IAEC/NCPA/2019-20

Consent: All authors declare that the manuscript has been reviewed and hereby provide consent to the corresponding author to make correspondence with the journal.

Acknowledgements: The authors express their sincere thanks to the principal and the management for the laboratory facilities and moral support. Gratitude is expressed to Dr. K. Sujatha, Asst. Professor in English, Department of Mathematics & Humanities for language editing.

REFERENCES

Abdelghany, T. M., Al-Rajhi, A.M.H., Al Abboud, M.A. et al. (2018). Recent advances in green synthesis of silver nanoparticles and their applications: About future directions. A Review. *BioNanoSci. 8*, 5-16. https://doi.org/10.1007/s12668-017-0413-3

Abdelghany, T.M., Maryam M. Hassan, Medhat A. El-Naggar, Mahmoud Abd El-Mongy (2020). GC/MS analysis of *Juniperus procera* extract and its activity with silver nanoparticles against *Aspergillus flavus* growth and aflatoxins production. *Biotechnology Reports, 27*, e00496. ISSN 2215-017X. https://doi.org/10.1016/j.btre.2020.e00496

Ankanna, S., Prasad, T.N.V.K.V., Elumalai, E.K., & Savithramma, N. (2010). Production of biogenic silver nanoparticles using *Boswellia ovalifoliolata* stem bark. *Digest Journal of Nanomaterials and Biostructures, 5*: 369-372.

Aslam, M., Kalyar M.A., & Raza, Z.A. (2019). Investigation of structural and thermal properties of distinct nanofillers-doped PVA composite films. *Polym Bull, 76*: 73–86. https://doi.org/10.1007/s00289-018-2367-1.

Cao, Y., Jin, R., & Mirkin, C. A. (2001). DNA-modified core-shell Ag/Au nanoparticles. *J Am Chem Soc, 123*: 7961-7962.

Clark, R. A. F. (1985). Cutaneous tissue repair: basic biologic considerations, *Journal of the American Academy of Dermatology, 13(5)*: 701–725.

Dakal, T. C., Kumar, A., Majumdar, R.S., & Yadav, V. (2016). Mechanistic Basis of Antimicrobial Actions of Silver Nanoparticles. *Front Microbiol, 7*: 1831. https://doi.org/10.3389/fmicb.2016.01831.

El-Rafie, H. M., & Hamed, M. (2014). Antioxidant and anti-inflammatory activities of silver nanoparticles biosynthesized from aqueous leaves extracts of four *Terminalia* species. *Adv Nat Sci Nanosci Nanotechnol, 5*: 1-11.

Florence, O., Afef, J., Tatiana, K., Vernessa, E., & Michael, C. (2013). Green synthesis of silver nanoparticles, their characterization, application and anti-bacterial activity. *International Journal of Environmental Research and Public health, 10*: 5221 – 5238. https://doi.org/10.3390/ijerph10105221

Gaaz, T.S., Sulong, A.B., Akhtar, M.N., Kadhum, A.A., Mohamad, A.B., & Al-Amiery, A. A. (2015). Properties and applications of polyvinyl alcohol, halloysite nanotubes and their nanocomposites. *Molecules 20*: 22833–22847.https://doi.org/10.3390/molecules201219884.

Ganash, M., Abdelghany, T.M. & Omar, A.M., (2018). Morphological and Biomolecules Dynamics of Phytopathogenic Fungi Under Stress of Silver Nanoparticles. *BioNanoSci. 8*, 566–573. https://doi.org/10.1007/s12668-018-0510-y

Gupta, B., Agarwal, R., & Alam, M.S. (2013). Preparation and characterization of polyvinyl alcohol-polyethylene oxide-carboxymethyl cellulose blend membranes. *J Appl Polym Sci, 127*: 1301–1308.https://doi/10.1002/app.37665

Hajialyani, M., Devesh Tewari, Eduardo Sobarzo-Sánchez, Seyed Mohammad Nabavi, Mohammad Hosein Farzaei, & Mohammad Abdollahi (2018). Natural product-based nanomedicines for wound healing purposes: therapeutic targets and drug delivery systems. *International Journal of Nanomedicine, 13*: 5023–5043.

Hasanin, M., Al Abboud, M.A., Alawlaqi, M.M. *et al.* (2021). Ecofriendly Synthesis of Biosynthesized Copper Nanoparticles with Starch-Based Nanocomposite: Antimicrobial, Antioxidant, and Anticancer Activities. *Biol Trace Elem Res*. https://doi.org/10.1007/s12011-021-02812-0

Hemant Kumar, N., Amit Kumar, S., Rajnish, S., Madan Lal, K., Harinarayan Singh, C., & Mahendra Singh, R. (2016). Pharmacological Investigation of the Wound Healing Activity of *Cestrum nocturnum* (L.) Ointment in Wistar Albino Rats. *Journal of Pharmaceutics 2016*; Article ID 9249040, 8 pages. https://dx.doi.org/10.1155/2016/9249040

Hsu, C.Y., Chan, Y.P., & Chang, J. (2007). Antioxidant activity of extract from *Polygonum cuspidatum. Biol Res, 40*: 13-21.

Im, A. R., Park, Y., & Kim, Y. S. (2010). Isolation and characterization of chondroitin sulfates from Sturgeon (*Acipenser sinensis*) and their effects on growth of fibroblasts. *Biol Pharm Bull, 33*: 1268–73.

Jain, J., Arora, S., Rajwade, J.M., Omray, P., Khandelwal, S., & Paknikar, K. M. (2009). Silver nanoparticles in therapeutics: development of an antimicrobial gel formulation for topical use. *Mol. Pharm 6*: 1388–401.

Kalaiarasi, K., Prasannaraj, G., Sahi, S.V., & Venkatachalam, P. (2015). Phytofabrication of biomolecule-coated metallic silver nanoparticles using leaf extracts of in vitro-raised bamboo species and its anticancer activity against human PC3 cell lines. *Turk J Biol, 39(2)*: 223–232.

Kanipandian, N., Kannan, S., Ramesh, R., Subramanian, P., & Thirumurugan, R. (2014). Antioxidant and cytotoxicity evaluation of green synthesized silver nanoparticles using *Cleistanthus collinus* extracts surface modifier. *Mater Res Bulletin, 49*: 494–502.

Kayalvizhi, T., Ravikumar, S., & Venkatachalam, P. (2016). Green Synthesis of Metallic Silver Nanoparticles Using *Curculigo orchioides* Rhizome Extracts and Evaluation of Its Antibacterial, Larvicidal, and Anticancer Activity. J Environ Eng, C4016002-1 -10. https://doi.org/10.1061/(ASCE)EE.1943-7870.0001098

Keshari, A. K., Ragini, S., Payal Singh, Virendra Bahadur Yadav, & Gopal Nath (2020). Antioxidant and antibacterial activity of silver nanoparticles synthesized by *Cestrum nocturnum*. *Journal of Ayurveda and Integrative Medicine, 11*: 37-44. https://doi.org/10.1016/j.jaim.2017.11.003.

Khan, A.U., Khan, M. & Khan, M.M. (2019). Antifungal and Antibacterial Assay by Silver Nanoparticles Synthesized from Aqueous Leaf Extract of *Trigonella foenum-graecum. BioNanoSci, 9*: 597–602. https://doi.org/10.1007/s12668-019-00643-x

Kharat, S.N., & Mendhulkar, V.D. (2016). *Synthesis Characterization and studies on Antioxidant activity of Silver Nanoparticles using Elephantopuss* caber leaf extract. *Mat Sci Eng, 62*: 719.

Kondo, T., & Ishida, Y. (2010). Molecular pathology of wound healing. *Forensic Science International, 203 (1–3)*: 93–98.

Kwan, K. H., Liu, X., To, M. K., Yeung, K. W., Ho, C. M., & Wong, K. K. (2011). Modulation of collagen alignment by silver nanoparticles results in better mechanical properties in wound healing. *Nanomed Nanotechnol, 7*: 497–504.

Lim, M., Kwon, H., Kim, D., Seo, J., Han, H., & Khan, S.B. (2015). Highly-enhanced water resistant and oxygen barrier properties of cross-linked polyvinyl alcohol hybrid films for packaging applications. *Prog Org Coat, 85*: 68–75. https://doi.org/10.1016/j.porgcoat.2015.03.005

Mandal, D., Bolander, M. E., Mukhopadhyay, D., Sarkar, G., & Mukherjee, P. (2006). The use of micro-organisms for the formation of metal nanoparticles and their application. *Appl Microbiol Biotechnol, 69*: 485. https://doi.org/10.1007/s00253-005-0179-3

Marcocci, L., Maguire, J., Droy-Lefaix, M., & Packer L. (1994). The nitric oxide-scavenging properties of Ginkgo biloba extract EGb 761. *Biochemical and Biophysical Research Communications, 201*: 748–755.

Mehta, B. K., Meenal Chhajlani, & Shrivastava, B. D. (2017). Green synthesis of silver nanoparticles and their characterization by XRD. Frontiers of Physics and Plasma Science, IOP Conf. Series: Journal of Physics: Conf. Series 2017; 836: 012050. https://doi.org/10.1088/1742-6596/836/1/012050.

Mohan Kumar, K., Sinha, M., Mandal, B.K., Ghosh, A.R., Siva Kumar, K., & Reddy, P. S. (2012). Green synthesis of silver nanoparticles using *Terminalia chebula* extract at room temperature and their antimicrobial studies. *Spectrochim. Acta A Mol Biomol Spectrosc, 91*: 228–233.

Muhammad, D. O., & Salih, N. A. (2012). Effect of application of Fenugreek (Trigonella foenum-graecum) on skin wound healing in rabbits. *AL-Qadisiya Journal of Vet.Med.Sci. 11 (2)*: 86-93.

Mukherjee, P.K., Verpoorte, R., & Suresh, B. (2000). Evaluation of in-vivo wound healing activity of *Hypericum Patulum* (Family: Hypericaceae) leaf extract on different wound model in rats. *Journal of Ethnopharmacology, 70 (3)*: 315–321.

Nanda, A., & Saravanan, M. (2009). Biosynthesis of silver nanoparticles from *Staphylococcus aureus* and its antimicrobial activity against MRSA and MRSE. *Nanomedicine 5*: 452–456. https://doi.org/10.1016/j.nano.2009.01.012

Okur Mehmet Evren, Ioannis D. Karantas, Zeynep Şenyiğit, Neslihan Üstündağ Okur, Panoraia I. Siafaka (2020). Recent trends on wound management: New therapeutic choices based on polymeric carriers. *Asian Journal of Pharmaceutical Sciences,*
15 (6): 661-684.

Oyaizu, M. (1986). Studies on products of the browning reaction. Antioxidative activities of browning reaction products prepared from glucosamine. *Japanese Journal of Nutrition, 44*: 307–315.

Parveen, M., Ahmad, F., Malla, A. M., & Azaz, S. (2016). Microwave-assisted green synthesis of silver nanoparticles from *Fraxinus excelsior* leaf extract and its antioxidant assay, Microwave-assisted green synthesis of silver nanoparticles from *Fraxinus excelsior* leaf extract and its antioxidant assay. *Appl Nanosci, 6*: 267–76.

Philip, D. (2011). *Mangifera indica* leaf-assisted biosynthesis of well-dispersed silver nanoparticles. *Spectrochim Acta Part A: Mol Biomol Spectroc, 78*: 327- 31.

Ponarulselvam, S., Panneerselvam, C., Murugan, K., Aarthi, N., Kalimuthu, K., & Thangamani, S. (2012). Synthesis of silver nanoparticles using leaves of *Catharanthus roseus* Linn. G. Don and their antiplasmodial activities. *Asian Pac J Trop Biomed, 2(7)*: 574–580.

Rahman, R., Dhruba, S.R., Ghosh, S. & Ranadip Pal (2019). Functional random forest with applications in dose-response predictions. *Sci Rep* **9,** 1628. https://doi.org/10.1038/s41598-018-38231-w

Rauwel, P., Kuunal, S., Ferdov, S., & Rauwel, E. (2015). Review on the Green Synthesis of Silver Nanoparticles and their morphologies Studied via TEM. *Adv Material Sci and Engg*. Article ID 682749, 9 pages. https://doi.org/10.1155/2015/682749.

Ruch, R.J., Cheng, S.J., & Klaunig, J.E. (1989). Prevention of cytotoxicity and inhibition of intercellular communication by antioxidant catechins isolated from Chinese green tea. *Carcinogenesis, 10*: 1003-1008.

Saha, K., Mukherjee, P.K., Das, J., Paul, M., & Saha, B. P. (1997). Wound healing activity of *Leucas lavendulaefolia* Rees. *Journal of Ethnopharmacology, 56*: 139-144.

Salem, W., Leitner, D. R., Zingl, F.G., Schratter, G., Prassl, R., Goessler, W., Joachim Reidl, & Stefan Schild (2015). Antibacterial activity of silver and zinc nanoparticles against *Vibrio cholerae* and enterotoxic *Escherichia coli*. *Int. J. Med Microbiol, 305*: 85–95.

Saumya, S., & Basha, P. (2011). Antioxidant effect of *Lagerstroemia speciosa Pers* (Banaba) leaf extract in streptozotocin-induced diabetic mice. *Indian J Exp Biol, 49*: 125-31.

Shakeel Ahmed, Mudasir Ahmad, Babu Lal Swami & Saiqa Ikram (2016). A review on plants extract mediated synthesis of silver nanoparticles for

antimicrobial applications: A green expertise. *Journal of Advanced Research, 7*: 17–28 https://doi.org/10.1016/j.jare.2015.02.007.
Shankar, S.S., Rai, A., Ahmad, A., & Sastry, M. (2004). Rapid synthesis of Au, Ag, and bimetallic Au core-Ag shell nanoparticles using Neem (*Azadirachta indica*) leaf broth. *J Colloid Interface Sci, 275(2)*: 496–502.
Sharma, V. K., Yngard, R.A, Lin, Y. (2009). Silver nanoparticles: green synthesis and their antimicrobial activities. *Adv Colloid Interface Sci, 145*: 83-96.
Sobha, K., Pradeep, D., Ratna Kumari, A., Verma, M.K., & Surendranath, K. (2017). Evaluation of therapeutic potential of the silver/silver chloride nanoparticles synthesized with the aqueous leaf extract of *Rumex acetosa*. *Scientific Reports, 7*: 11566.https://doi.org10.1038/s41598-017-11853-2
Sondi, I., & Sondi, B. S. (2004). Silver nanoparticles as antimicrobial agent: a case study on *E. coli* as a model for Gram-negative bacteria. *J Colloid Interface Sci 275*: 177-182.
Trease, G.E., & Evans, W.C. (1989). Pharmacognosy. 11th ed. Bailliere Tindall: Cassell and Collier Macmillan Publishers.
Udupa, A.L., Kulkarni, D.L., & Udupa, S. L. (1995). Effect of *Tridax procumbens* extracts on wound healing. *International Journal of Pharmacognosy, 33(1)*: 37–40.
Udupa, S.L., Udupa, A.L., & Kulkarni, D. R. (1994a). Anti-inflammatory and wound healing properties of Aloe vera. *Fitoterapia, 65(2)*: 141-145.
Uparelia, J. P., Chatterjee, A. K., Dasgupta, S.P., & Mukherji, S. (2008). Strain specificity in antimicrobial activity of silver and copper nanoparticles. *Acta Biomater, 4*: 707-716.
Yakabe, Y,, Sano, T., Ushio, H., & Yasunaga, T. (1980). Kinetic studies of the interaction between silver ions and deoxy ribo nucleic acid. *Chem Lett, 4*: 373-376.
Yang, J., Guo, J., & Yuan, J. (2008). In vitro antioxidant properties of rutin. LWT—*Food Science and Technology, 41(6)*: 1060–1066.
Yoon, K.Y., Byeon, J. H., Park, J. H., & Hwang, J. (2007). Susceptibility constants of *Escherichia coli* and *Bacillus subtilis* to silver and copper nanoparticles. *Sci Total Environ, 373*: 572-575.